



# Towards hybrid one-pot/one-electrode Pd-NPs-based nanoreactors for modular biocatalysis

M. Koch<sup>a</sup>, N. Apushkinskaya<sup>b</sup>, E.V. Zolotukhina<sup>c</sup>, Y.E. Silina<sup>b,\*</sup>

<sup>a</sup> INM-Leibniz Institute for New Materials, Campus D2 2, 66123 Saarbrücken, Germany

<sup>b</sup> Institute for Biochemistry, Centre of Human and Molecular Biology, University of Saarland, Campus B 2.2, 66123 Saarbrücken, Germany

<sup>c</sup> Institute of Problems of Chemical Physics, Russian Academy of Science, 142432 Chernogolovka, Moscow Region, Russia

## ARTICLE INFO

### Keywords:

One-pot/one-electrode nanobiosensor  
Multiplexed analysis  
Small molecular weight bioanalytes  
Read-out mode

## ABSTRACT

Here, fundamental aspects affecting template-assisted engineering of oxidase-associated peroxide oxidation co-catalysis of the modeled microanalytical system based on the hybrid palladium nanoparticles (Pd-NPs) with tailored functional properties were studied. By an accurate tuning and validation of the experimental setup, a modular Pd-NPs-doped one-pot/one-electrode amperometric nanobiosensor for advanced multiplex analyte detection was constructed. The specific operational conditions (electrochemical read-out mode, pH, regeneration procedure) of the modular one-pot/one-electrode nanobiosensor allowed a reliable sensing of L-lactate (with linear dynamic range, LDR = 500  $\mu$ M – 2 mM,  $R^2$  = 0.977), D-glucose (with LDR = 200  $\mu$ M – 50 mM,  $R^2$  = 0.987), hydrogen peroxide (with LDR = 20  $\mu$ M – 100 mM,  $R^2$  = 0.998) and glutaraldehyde (with LDR = 1 – 100 mM,  $R^2$  = 0.971). In addition, mechanistic aspects influencing the performance of Pd-NPs-doped one-pot/one-electrode for multiplex analyte sensing were studied in detail. The designed one-pot/one-electrode amperometric nanobiosensor showed a thin layer electrochemical behavior that greatly enhanced electron transfer between the functional hybrid layer and the electrode. Finally, a specific regeneration procedure of the hybrid one-pot/one-electrode and algorithm towards its usage for modular biocatalysis were developed. The reported strategy can readily be considered as a guideline towards the fabrication of commercialized nanobiosensors with tailored properties for advanced modular biocatalysis.

## 1. Introduction

Cascade nanobiocatalysis that employs more than two consecutive bioreactions in one-pot is a promising biotechnology and challenging engineering task [1,2]. Contrary to the multi-steps reactors, cascade biocatalysis allows avoiding the isolation of intermediate products, helps to eliminate accumulation of toxic reagents and reduces fabrication and operation costs. For this goal, principles of modular nanobiocatalysts can be utilized [3]. Modularity can be achieved by the design of nanoreactors. Notably, in modular nanobioreactors all multi-component system elements should be interchanged for functional flexibility in a fully controlled and predicted manner.

With regards to nanobiosensors development, a modular approach can be realized, if enzyme immobilization occurs by a reproducible and highly-controlled technique. However, numerous reports to produce oxidase-based bio- and nanobiosensors consisting up to six or seven components can be found [4,5]. In fact, this makes the manufacture of

those bioanalytical devices really complex, highly irreproducible, very time consuming and quite expensive. Most of them will probably never be commercialized. To the best of our knowledge, almost no attempts were done to construct oxidase-based nanobiosensors with tailored segmental blocks for the detection of multiplexed analytes by a single one-pot/one-electrode. Apparently, this would require an essential fundamental knowledge on the template-assisted engineering allowing the fabrication of functional nanobioreactors with tailored and predicted properties [4]. Instead, several expensive arrays of integrated nanobiosensors with different architecture, synthesis strategy, complex interface and read-out modes were proposed [6,7].

In the majority, the fabrication of conventional nanobiosensors is based on layer-by-layer (LbL) approach [8]. Despite the simplicity of LbL approach it suffers from low synthesis reproducibility and requires the usage of toxic cross-linker agents (i.e. glutaraldehyde) resulting in impurities and inhomogeneity within an active bioreceptor layer. In addition, biosensors with the LbL architecture are limited to

\* Corresponding author.

E-mail addresses: [yuliya.silina@uni-saarland.de](mailto:yuliya.silina@uni-saarland.de), [yuliya.silina@gmx.de](mailto:yuliya.silina@gmx.de) (Y.E. Silina).

<https://doi.org/10.1016/j.bej.2021.108132>

Received 26 May 2021; Received in revised form 4 July 2021; Accepted 6 July 2021

Available online 8 July 2021

1369-703X/© 2021 The Author(s).

Published by Elsevier B.V. This is an open access article under the CC BY-NC-ND license

(<http://creativecommons.org/licenses/by-nc-nd/4.0/>).

electrostatic interactions [9] resulting in the leaching of functional layers, *i.e.* mediator, bioreceptor or polymer (used to protect water soluble protein). More importantly, nanobiosensors designed by LbL protocols may contain numerous unreacted compounds, which can result in the cascade of unpredictable reactions. Hence, the usage of LbL-designed sensors for modular nanobiocatalysis is not a trivial engineering task. More importantly, approaches towards reliable, tailored and reproducible synthesis, simple electrochemical and bioelectronic interface in multifunctional nanobiosensors manufacturing are currently lacking [10].

One of the most employed strategies in the production of multi-step nanoreactors is a covalent simultaneous co-immobilization of several free enzymes from the cocktail mixture on nano-based templates [3]. However, this approach demonstrates a competitive behavior of the multiple bioreceptors during their attachment to the active sides of cross-linker agents, low synthesis reproducibility and low enzyme activity *versus* conventional single-enzyme designed nanobiosensors [11–13].

To address these challenges, recently, a novel one-step electrodeposition platform towards the production of nanobiosensors with tailored and controlled architecture was proposed [14]. This approach demonstrated a superior controllable synthesis, excellent chemical, storage and mechanical stability as compared to the LbL analogs. In addition, by methods of quantum chemistry a capsular model of the sensing layer formed on the surface of screen printed electrodes modified with graphene oxide, mainly composed of encapsulated enzyme and water molecules incorporated into a metal polymer scaffold, was revealed [15].

The next step in the development of the electroplated nanobiosensors with tailored properties would be the construction of modular one-pot analytical devices [16] for multiplexed analysis.

Here, a one-pot/one-electrode nanobiosensor was developed for advanced multiplex bioanalyte detection. Multi-enzyme immobilization on a single screen printed electrode (SPE) was achieved by consequence electroplating performed in a step by step manner from the solution containing targeted enzymes (glucose oxidase, GOx and lactate oxidase, LOx), Nafion (binding agent/enzymatic protective layer) and palladium electrolyte. This procedure enables the formation of several functional nanoparticulated levels on the same electrode, *i.e.*, palladium nanoparticles (Pd-NPs)-Nafion-doped GOx distributed between Pd-NPs-Nafion-doped LOx. This architecture provides the channeling-like effect for analytes to the targeted nanoparticulated enzymatic level, enhances their diffusion and electron transport between the electrode and active sides of the bioreceptors. Finally, the protocol towards the usage of a one-pot/one-electrode nanobiosensor after enzyme deactivation for facile analysis of hydrogen peroxide and glutaraldehyde in a separate electrochemical read-out mode was developed.

## 2. Experimental part

Electrodes, chemicals and used reagents are detailed in the [Supplementary Material](#).

### 2.1. Template preparation

The synthesis of Pd-NPs-based templates was carried out from Pd-electrolyte [17] by electroplating on the surface of SPE at different current (varied from  $\mu\text{A}$  to mA range) and deposition time (from 30 s to 10 min) using the one-channel biologic Potentiostat PalmSens4 (PalmSens, Utrecht, Netherlands).

To compare the performance of 3D-dimensional Pd-NPs-doped templates, SPEs modified by Pd-ink and 2D-sputtered Pd-foil (20 nm) were used (see [ESI](#)).

### 2.2. Preparation and electrochemical characterization of Pd-NPs-doped one-step and multi-step designed one-pot/one-electrode nanobiosensors

First, the encapsulation of bioreceptors (GOx or LOx) together with Nafion (further Naf) was carried out on the surface of SPEs by one-step approach according to the earlier reported protocol [18]. GOx and LOx stock solutions were prepared in phosphate buffer at the level from 1 mg/mL to 18 mg/mL.

Furthermore, the deposition of bioreceptors (GOx followed by LOx) on the surface of Pd-NPs modified SPE was conducted in the multi-step manner from the corresponding multicomponent electrolyte-enzyme solutions in chronopotentiometric (CP) mode. This design will be further referred as “one-pot/one-electrode nanobiosensor” and consists of several levels: first – pure Pd-NPs, the second – a mixture of Pd/GOx/Naf and the third – Pd/LOx/Naf. It is assumed that the second and third organic-inorganic hybrid layers will be homogeneously distributed between the gaps of the first layer (pure Pd-NPs).

Regardless the design all Pd-NPs-doped nanobiosensors were tested in cyclic voltammetry (CV) at a scan rate of 20 mV/s. Electrodeposition and testing of nanobiosensors were carried out on the one-channel biologic Potentiostat PalmSens4 (PalmSens, Utrecht, Netherlands). The preparation route and read-out supplied by the nanobiosensors was controlled by the PSTrace Software (PalmSens, Utrecht, Netherlands).

### 2.3. Oxygen mini-sensor study

To estimate the impact of glutaraldehyde (GLU) addition on bioreceptor activity, an OXR430 retractable needle-type fiber-optic oxygen minisensor (PyroScience GmbH, Aachen, Germany) was utilized.

### 2.4. Laser desorption ionization mass-spectrometry (LDI-MS)

To ensure enzyme encapsulation from the multiple electrolyte solution on the surface of SPEs, the corresponding co-factors (GOx employs Flavin dinucleotide, FAD; LOx – Flavin mononucleotide, FMN) were monitored by atmospheric pressure laser desorption ionization mass spectrometry (AP-LDI-MS) according to a recently reported protocol [18]. All experiments were conducted on a Bruker (Bremen, Germany) Esquire HCT+3D ion trap mass spectrometer equipped with a Nd:YAG solid-state laser (355 nm, 200 Hz).

### 2.5. Scanning electron microscopy (SEM)

SEM images were captured on a Quanta (Hillsboro, OR, USA) 400 FEG system equipped with an EDAX (Mahwah, NJ, USA) Genesis V 6.04 X-ray spectral analysis system, at an accelerating voltage of 10 keV. The image size was  $1024 \times 884$  pixels.

### 2.6. TEM study

To verify a truly encapsulation of the bioreceptor during electroplating *versus* surface adsorption, a set of TEM studies of Pd-NPs-modified SPEs was conducted. For analysis small pieces of the functional sensing layer were released by scratching using sandpaper P180. An ethanol droplet was placed on a holey carbon grid (Plano, Wetzlar, type S147-4) to disperse the abrasion on the supporting carbon film. Bright field TEM images were obtained at 200 kV accelerating voltage using a JEOL (Akishima, Tokyo, Japan) JEM 2100 Lab<sub>6</sub> microscope (HR pole piece) equipped with a Gatan (Pleasanton, CA, USA) Orius SC1000 CCD camera.

### 3. Results and discussion

#### 3.1. Towards nanoreactors for modular biocatalysis: proof of concept and operating principles of Pd-NPs-based one-pot/one-electrode nanobiosensors

By a comprehensive study of the geometry and size of the hybrid Pd-NPs-dopants, an established impact of electrodeposition parameters on their functional properties and an optimization of read-out platform has become possible to construct and validate one-pot/one electrode nanobiosensor with switchable modules for advanced multiplex analyte detection, *viz.* L-lactate, D-glucose, hydrogen peroxide and glutaraldehyde as a case study, Fig. 1.

The synthesis of one-pot/one-electrode designed nanobiosensors for multiple bioanalyte detection is a fully instrumentally controlled procedure (Fig. 1A). Multi-enzyme immobilization on a single electrode can be achieved by electroplating performed in a consequence manner from the solution containing enzyme of interest, Nafion and palladium electrolyte (see EDX spectra, ESI, Fig. S1). One of the most crucial steps is to

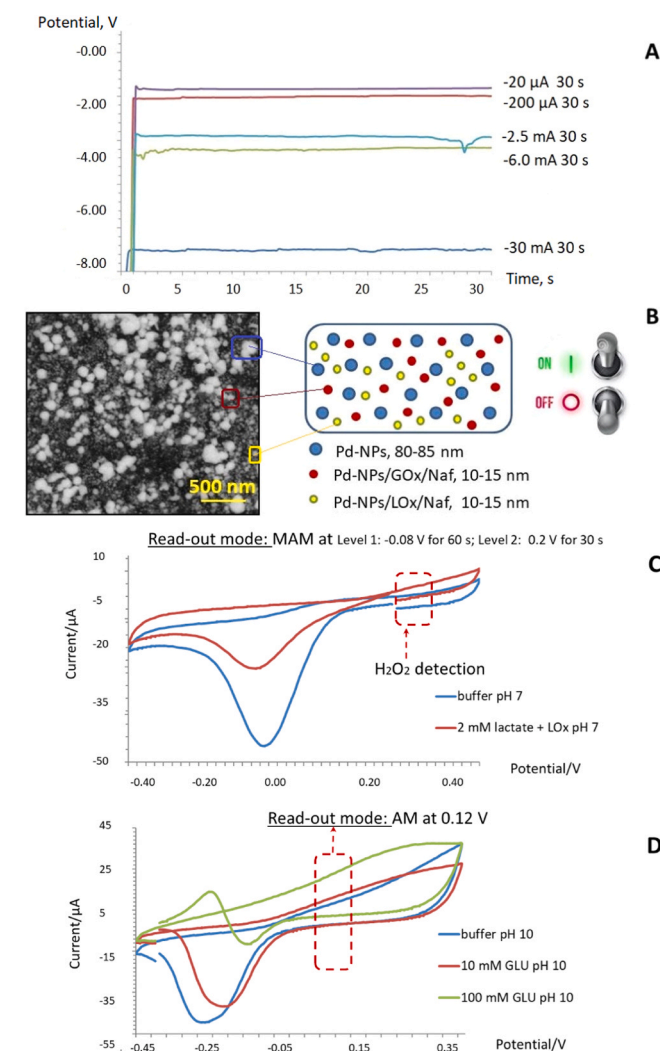


**Fig. 1.** Workflow of the modular one-pot/one-electrode Pd-NPs-doped nanobiosensor: (A) fully instrumentally controlled fabrication in chronopotentiometric (CP) mode; (B) SEM image and scheme of the hybrid one-pot/one-electrode Pd-NPs-doped nanobiosensor. Note: “ON/OFF” option illustrates the possibility of the controlled switching between functional pure (Pd-NPs) and hybrid nanoparticles (Pd-NPs/GOx/Naf or Pd-NPs/LOx/Naf) depending on their operational mode (C,D) – different read-out modes for H<sub>2</sub>O<sub>2</sub>-sensing (C) and glutaraldehyde (GLU) (D).

define template engineering settings of the segmental blocks (Fig. 1B) to provide a predicted sensor response. Thus, depending on the morphology, size, distribution and surface chemistry of the functional nanoparticles (see Sections 3.2–3.4) a different analytical response can readily be obtained. Also, it is necessary to optimize the electrochemical read-out mode allowing a separate detection of the targeted analyte (Fig. 1C,D).

The next goal of this study was to define optimal synthesis parameters of one-pot/one-electrode nanobiosensors providing the required analytical merit and to establish its certain electrochemical read-out depending on the targeted analyte. The chosen operational conditions will allow a reliable switch between the analytes (L-lactate, D-glucose, hydrogen peroxide and glutaraldehyde) by the type of the immobilized enzyme (GOx or LOx), pH, polarization mode and specific sensor regeneration procedures (see next sections).

#### 3.2. Key parameters affecting the performance of electrode

##### 3.2.1. Impact of nanobiosensor composition and polarization mode

Selective detection of D-glucose and L-lactate can be realized by the use of corresponding oxidases (GOx/LOx). The co-product of these reactions is hydrogen peroxide:



which is expected to be detected by Pd-NPs.

Therefore, it was important to define the electrochemical read-out mode for a reliable detection of H<sub>2</sub>O<sub>2</sub> as a product of enzymatic activity by Pd-NPs. During the set of CV experiments we found that the synthesis mode of Pd-NPs dramatically affects their electrochemical response in the cathodic range of potentials, see Fig. 2. It is assumed, that the observed effect is connected with the size of Pd-NPs and the change in their surface chemistry, *viz.* the formation of different amount and types of Pd-oxides [19].

On the contrary, regardless the synthesis conditions of Pd-NPs, the signal obtained at the anodic range (at 0.2 V) was different only in terms of the basic line intensity (basic current), see Fig. 2. Briefly, the more current was applied during synthesis, the higher the basic line of the Pd-NPs-based sensor was generated. Hence, it appears to be possible to detect H<sub>2</sub>O<sub>2</sub> as an individual analyte or the product of enzymatic reaction by Pd-NPs in the anodic range of potentials. However, to refresh the electrode surface, it is highly necessary to reduce Pd-oxides formed during anodic polarization. For this goal, we optimized the following

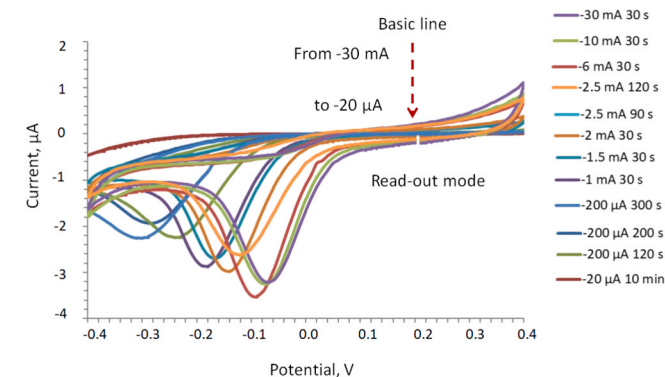


**Fig. 2.** CV curves obtained at 20 mV/s in a phosphate buffer (pH 6.98) from pure Pd-NPs produced at different electroplating conditions (deposition time and current).



double step procedure: the first step is a polarization at the cathodic peak potential to reduce Pd-oxides, the second step is a polarization at the anodic potential in the range of 0.2 V to detect/record the current related to hydrogen peroxide decomposition. This applied multi-step amperometric (MAM) read-out mode (the first step is a polarization at the cathodic peak potential ( $-0.08$  V) to reduce Pd-oxides, the second step is a polarization at 0.2 V to detect  $\text{H}_2\text{O}_2$  oxidation current) results in a faster  $\text{Pd}_x\text{O}_y$  reduction and thus regeneration of the surface for a reliable peroxide sensing at the anodic range.

Standardization of the basic line at the applied MAM conditions will allow us peroxide sensing at pH 7 not only as a product of oxidase's activity (low concentration range) but also as an individual component at much higher concentration levels (see Section 3.6). The sensing of glutaraldehyde by the same Pd-NPs can be realized by the change of pH and a different applied electrochemical read-out mode (see Section 3.5).

### 3.2.2. Tailoring of sensing properties of Pd-NPs-doped nanoreactors via synthesis mode

To verify the effect of Pd-NPs 3D-surface on the analytical performance of our nanobiosensors, we compared the signal obtained from Pd-NPs (synthesized at  $-2.5$  mA, 30 s with a thickness of nanoparticulated layer 20 nm) in the presence of 1 mM  $\text{H}_2\text{O}_2$  with the signal recorded from 2D-structured electrodes modified by sputtered Pd-foil (thickness of 20 nm) and Pd-ink. As it is seen, the signal intensity obtained from 3D-Pd-NPs modified nanoelectrode was several times higher versus the response recorded from 2D-electrodes modified by Pd-foil or Pd-ink, ESI, Fig. S2. Hence, by this experiment we demonstrated that the electrochemical signal, when employing 3D-Pd-NPs, is a factor of the surface area. Based on the obtained results, in further experiments Pd-NPs-doped electrodes were utilized.

Next, it was necessary to define the optimal synthesis conditions of pure Pd-NPs as a template-assisted module driving further self-assembling formation of enzyme-contained layers to construct

enzymatic nanoreactors with optimized sequences. For this goal, we performed an electrochemical tuning of Pd-NPs depending on synthesis parameters and evaluated their analytical merit, Fig. 3. Significantly, the increase of deposition time mostly impacts the size of Pd-NPs formed at  $-2.5$  mA (see Fig. 3A), resulting in their agglomeration and decrease of the electroactive surface area. In contrast, the change of current is affecting both parameters, i.e., the amount and size of Pd-NPs, Fig. 3B.

Experimentally, it was found that at low deposition currents ( $\mu\text{A}$ ) monodisperse Pd-NPs can be formed. This architecture of the template can be attractive for further immobilization of enzymes due to the provided gap-channeling design. The formed gaps can readily be filled by enzyme-contained structures in a tailored manner. Unfortunately, the analytical performance of monodisperse Pd-NPs produced at low deposition currents ( $\mu\text{A}$ ) to  $\text{H}_2\text{O}_2$  decomposition was very poor, Fig. 3C. This result can be explained by an insufficient amount of the formed Pd-NPs that impacts the entire sensor response to  $\text{H}_2\text{O}_2$ . In other words, the change of morphology, size, dimensionality and distance between Pd-NPs will result in a different sensor performance, Fig. 3C–E.

In summary, the best sensitivity of  $2377 \mu\text{A}/\mu\text{mol}$  was obtained from Pd-NPs synthesized at  $-2.5$  mA for 30 s, see Fig. 3D,E. The increase of current or deposition time was accompanied by a loss in  $\text{H}_2\text{O}_2$  sensitivity possible due to a decrease in surface area of 3D-formed Pd-NPs. The doping of Pd-NPs by organic component (immobilization from GOx-Naf-contained solution) leads to a significant loss in the sensor response. Thus, the opposite trend as established above for pure Pd-NPs was recorded for their organic-inorganic hybrids (OIH), (Fig. 3F). With increase of deposition time from 30 s to 120 s the sensitivity to  $\text{H}_2\text{O}_2$  decomposition by Pd/GOx/Naf-doped OIH increases (electroactive area of the hybrid Pd-NPs formed at  $-2.5$  mA for 120 s is equivalent to electroactive area of pure Pd-NPs produced at  $-2.5$  mA for 30 s). These results highlight that the interaction between Pd-NPs and enzymes must be carefully engineered (see Section 3.3).

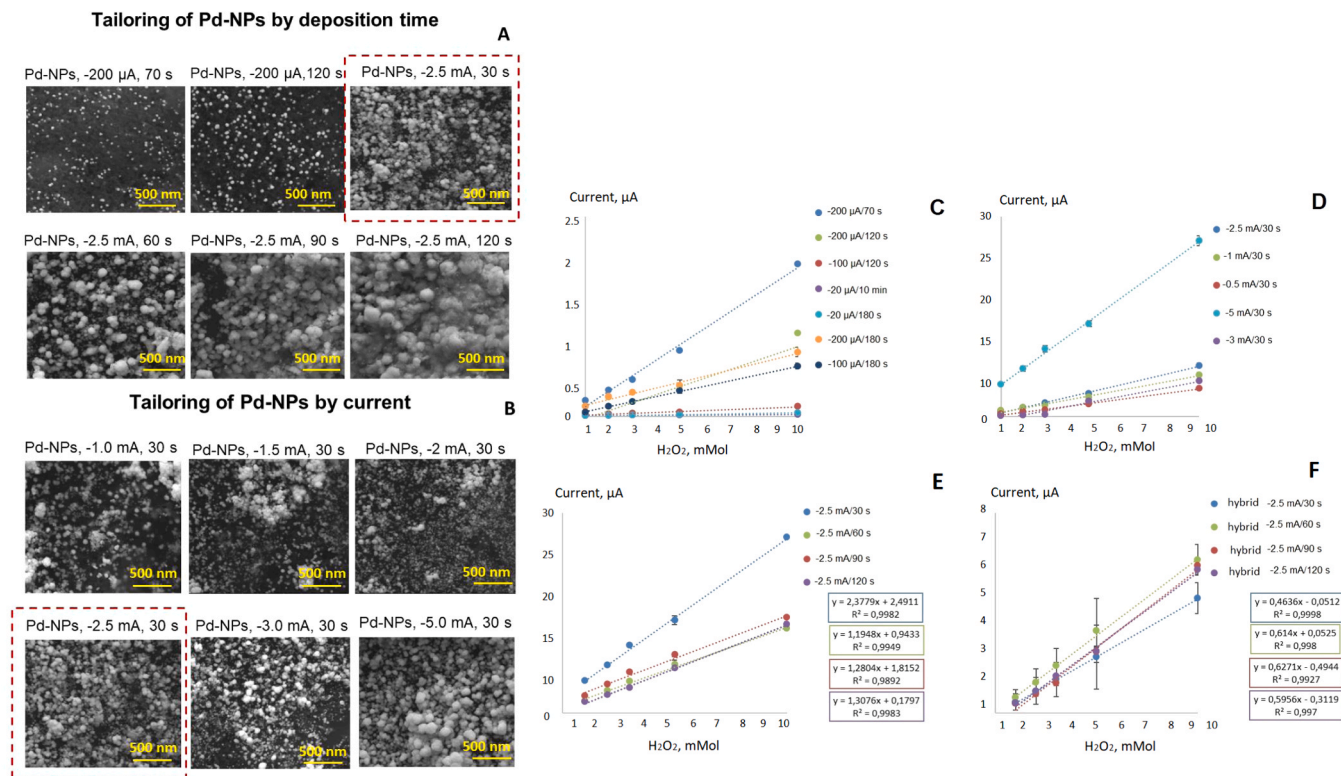


Fig. 3. (A,B) – SEM images obtained from Pd-NPs produced at various deposition times (A) and currents (B). The performance of pure Pd-NPs (C–F) and Pd/GOx/Naf-doped hybrids (D) towards  $\text{H}_2\text{O}_2$  sensing estimated in the analytical range of concentrations at pH 6.98: (C) – Pd-NPs produced at low ( $\mu\text{A}$ ) current; (D) – Pd-NPs synthesized at various current (mA) and 30 s; (E) – pure Pd-NPs and Pd/GOx/Naf hybrid (F) produced at  $-2.5$  mA and various deposition time.

### 3.3. Technological compromise by the design of Pd-NPs-doped nanostructures for advanced bioanalyte sensing

#### 3.3.1. Impact of bioreceptor concentration on nanobiosensor performance

Further, it was necessary to define a technological compromise between the design of 3D Pd-NPs-based structures protecting the Nafion and enzymes from a non-controlled leakage and, at the same time, providing the controlled release of bioreceptor in the presence of analyte. At this step we claimed to find out the optimal distance between NPs, their diameter and concentration of enzyme, which is necessary to provide the required analytical merit. A slight difference in the structure of these hybrids will affect the catalytic activity of enzymes and the transport rates of bioanalytes.

In this regards, we varied the concentration of bioreceptor (GOx as a case study) that is planned to be immobilized via electroplating with Pd-NPs and Nafion from the multicomponent electrolyte. Interestingly, increasing of GOx concentration from 1 mg/mL to 9 mg/mL was accompanied by a simultaneous increase of generated voltage and sensor sensitivity, see Fig. 4A,B.

However, a further increase of GOx concentration to 12 mg/mL and 18 mg/mL resulted in a significant lack in sensor sensitivity. This trend was confirmed by SEM studies, Fig. 4C. The observed phenomenon can be explained by a too high concentration of organic component in the electrolyte resulting in the formation of an adsorptive OIH layer instead of the desired 3D-core shell/capsule-like structure. In addition, the increase of GOx concentration in the multiple electrolyte solution from 1 mg/mL to 18 mg/mL was accompanied by a simultaneous increase of voltage during electroplating, i.e., from  $-3.8 \pm 0.37$  V to  $-6.9 \pm 0.21$  V (see Fig. 4A). In general, if the voltage during enzyme co-deposition reaches the level above  $-5.23 \pm 0.21$  V, a significant lack of sensor response can be expected due to conformational changes in the structure of bioreceptor. Hence, the concentration of the used enzymes mustn't exceed the level of 5–9 mg/mL.

#### 3.3.2. Impact of the hybrid Pd-NPs-Nafion-doped structure on enzyme retention and nanobiosensor performance

To set up an optimal design of the hybrid Pd-NPs-Nafion-doped structure to retain/store the enzyme, and to elucidate the diffusion limitations in the system, to find an optimal ratio between Pd-NPs density and size of NPs, it was necessary to explore Pd-NPs-doped nanobiosensors with different architectures. During manufacturing of one-step designed nanobiosensors their morphology and the size of NPs was carefully monitored by SEM and TEM analyses followed by evaluation of the response supplied by these structures in the presence of analyte. Importantly, apart from the basic line, sensitivity (Table 1) and linear dynamic range (LDR), this nanobioengineering step also affects the mechanical stability of the formed functional layer (*data not shown*) and accuracy supplied by these nanoanalytical devices. The performed specificity test didn't reveal a significant interference from D-fructose during detection of D-glucose by Pd-NPs/GOx/Naf nanobiosensors regardless their design (ESI, Fig. S3).

With regards to nanobiosensor engineering aspect, the decrease of both parameters (current and deposition time) during formation of organic-inorganic hybrids (OIH) was accomplished by a significant lack in response possibly explained in terms of insufficient and incomplete retention of enzyme at these conditions. A decrease of current from  $-2.5$  mA to  $-1$  mA and an increase of deposition time from 30 s to 120 s during manufacturing of nanobiosensors was accompanied by an increase of Pd-NPs-doped size and loss in their sensitivity from  $162 \pm 8$   $\mu$ A/ $\mu$ mol ( $-2.5$  mA for 30 s) to  $128 \pm 12$   $\mu$ A/ $\mu$ mol ( $-1$  mA for 120 s). The increase of both parameters, i.e., current and deposition time ( $-5$  mA, 120 s) has gone along by a complete loss in sensor activity that is explained by the formation of too big Pd-NPs and the absence of the entrapped enzyme, see also ESI, Fig. S4.

These dependencies were confirmed by TEM studies. Thus, hybrid Pd-NPs produced at  $-2.5$  mA for 30 s were surrounded by an organic shell, see Fig. 5. Further increase of deposition current and time resulted

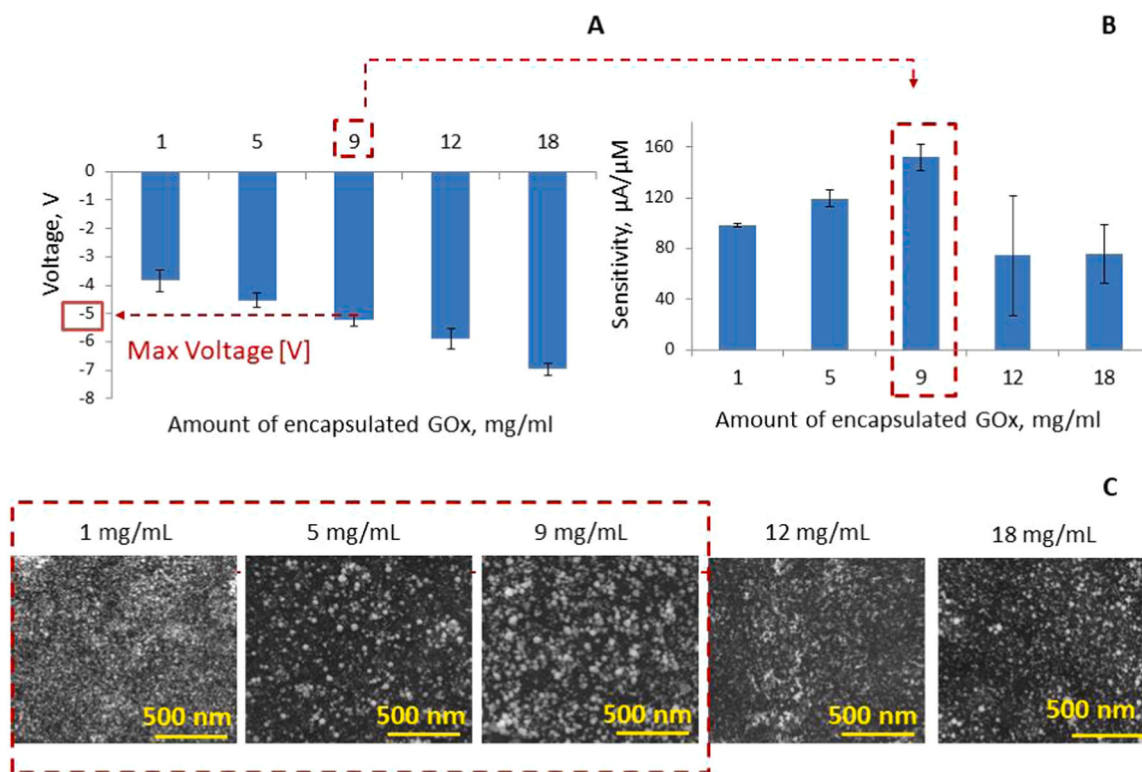


Fig. 4. Tailoring of analytical performance of 3D Pd-NPs-doped nanobiosensors by the amount of co-deposited enzyme (deposition parameters  $-2.5$  mA for 30 s): A – electrochemical responses recorded during fabrication of one-step nanobiosensors, B – sensitivity (B) of these sensors estimated in the presence of glucose. C – SEM images depending of one-step designed nanobiosensors produced at different concentration of GOx.

**Table 1**

The impact of one-step nanobiosensor design (Pd/GOx/Naf) on their performance<sup>a</sup>.

| Design                         | LDR, mM                            | Sensitivity, $\mu\text{A}/\mu\text{Mol}$ | Basic line, $\mu\text{A}$     | Accuracy, % |
|--------------------------------|------------------------------------|--|-------------------------------|-------------|
| -2.5 mA, 30 s<br>5 mg/mL (GOx) | 0.2–100                            | 115                                      | $2.90 \cdot 10^{-1} \pm 0.11$ | 92          |
| -5 mA, 30 s<br>5 mg/mL (GOx)   | 5–50                               | 49                                       | $1.20 \cdot 10^{-1} \pm 0.12$ | 87          |
| -2.5 mA, 30 s<br>9 mg/mL (GOx) | 0.2–100                            | 160                                      | $5.50 \cdot 10^{-1} \pm 1.27$ | 96          |
| -5 mA, 120 s<br>9 mg/mL (GOx)  | No release of enzyme/not entrapped | No release of enzyme/not entrapped       | $3.05 \cdot 10^{-1} \pm 0.17$ | –           |
| -2.5 mA, 90 s<br>9 mg/mL (GOx) | 1–5                                | 468                                      | $4.83 \cdot 10^{-1} \pm 0.32$ | 89          |
| -1.0 mA, 30 s<br>9 mg/mL (GOx) | 1–10                               | 40                                       | $7.5 \cdot 10^{-1} \pm 0.11$  | 94          |

<sup>a</sup> Estimated in the presence of glucose.

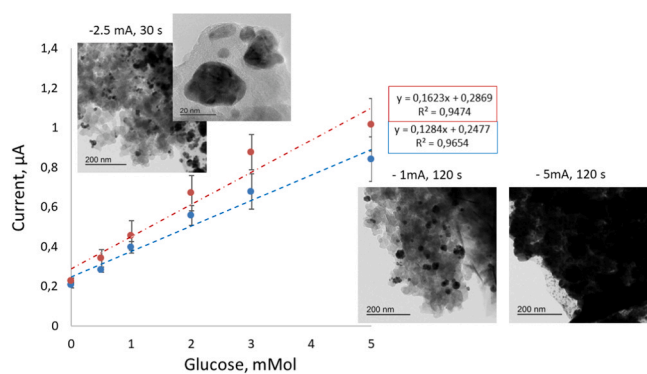


**Fig. 5.** Calibration curves obtained from one-step designed Pd/GOx/Naf nanobiosensors (in the presence of glucose) fabricated at different currents and deposition times: red line – synthesized at  $-2.5$  mA for 30 s; blue line – synthesized at  $-1$  mA for 120 s (GOx stock 9 mg/mL). Note – the calibration curve for sensor produced at  $-5$  mA for 120 s cannot be shown (enzyme is not entrapped/retained). Inserts – TEM images. (For interpretation of the references to color in this figure legend, the reader is referred to the web version of this article.)

in the increase of inorganic Pd-NPs content and a decrease of organic (bioreceptor-contained) component. As a result, a lack of electrochemical activity from the hybrid nanobiosensors produced at these conditions was detected. The current increase to  $-5$  mA leads to the formation of an adsorptive-like OIH layer that is not properly retained on Pd-NPs and can rapidly elute after immersion in buffer or sample solutions.

### 3.4. Mechanistic aspects of sensing by one-pot/one-electrode nanobiosensor

In order to verify a reliable LOx and GOx immobilization (as a second level on the surface of Pd-NPs modified SPE/GO) we conducted LDI-MS studies. Mass spectra received after immobilization of LOx (Fig. 6A) exhibited by riboflavin (RbF) corresponding species (RbF is a fragment of Flavin mononucleotide (FMN) – LOx co-factor), viz.  $[\text{M}+\text{H}]^+$  at  $m/z$  377.5 and  $[\text{M}+2]^+$  seen at  $m/z$  378.5, that was in line with results

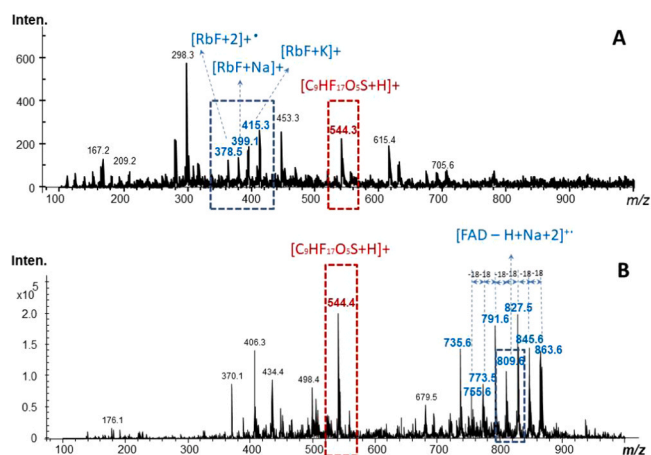


**Fig. 6.** LDI-MS spectra obtained in positive ionization mode from Pd-NPs modified SPE/GO after separate LOx (estimated as FMN co-factor) (A) and GOx (estimated as FAD) (B) immobilization with Nafion (at  $-2.5$  mA for 30 s), laser fluence 45%.

reported by MALDI-MS [20]. Similar behavior during ionization was detected for glucose oxidase (employs FAD as a co-factor), see Fig. 6B. Thus, by LDI-MS we approved the successful immobilization of both enzymes together with Nafion (at  $m/z$  544) and Pd-NPs.

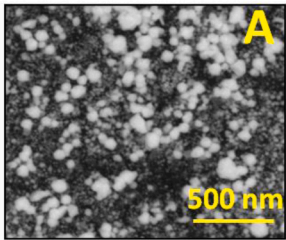
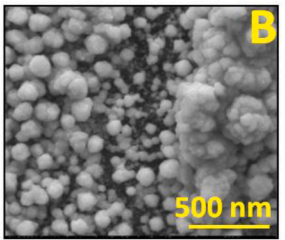
Further, it was necessary to define the compromise in design of one-pot/one-electrode nanobiosensor (Pd-NPs, 1-st level, Pd/LOx/Naf, 2-d level, and Pd/GOx/Naf, 3-d level) providing a similar performance towards consecutive lactate, glucose and hydrogen peroxide sensing compared to individually immobilized functional layers. Thus, the morphology of Pd-NPs and the architecture of the active layer (see sections above) had a significant impact on the entire response of one-step nanobiosensors. A similar effect can be expected in three Pd-NPs-based layered structures. To verify this fact, next we produced Pd-NPs-assisted one-pot/one-electrode (three layered structures) at slightly different electroplating condition, see Table 2.

Based on the obtained above dependencies regarding deposition of functional enzyme-contained sensing level (one-step design) a current of  $-2.5$  mA applied for 30 s was used. SEM studies (see insert Table 2) revealed the thickness of the functional layer of one-pot/one-electrode is about 15–20 nm that can significantly improve the communication between the redox center of bioreceptor and the electrode surface. The increase of deposition current (up to  $-5$  mA) and time (from 30 s to 120 s) leads to an agglomeration of the layers together resulting in the formation of a thicker functional film (see SEM images, inserts in Table 2). This architecture didn't provide enough space between the functional NPs and represents more likely a layer-by-layer nanoparticulated architecture. We assume that due to the increased thickness of the entire functional layer on the electrode surface the linear dynamic range (LDR) obtained from these structures was not optimal. Thus, one of the main difficulties in bioelectrochemistry is to properly connect enzymes onto the surface to bring the redox center of bioreceptor close to the electrode surface [5]. Hence, the advanced analytical merit of one-pot/one-electrode designed at  $-2.5$  mA for 30 s towards small molecular weight compounds detection can be explained by the formation of a thin functional Pd-NPs-doped film on the electrode that increases the rate of electron transfer. Pd-NPs as an electrocatalyst in nanobiosensor design support the efficient sensing of hydrogen peroxide released during specific enzymatic reaction.

Moreover, the design of the produced nanobiosensor has an advantage versus conventional LbL-produced biosensors using glutaraldehyde (GLU) in the composition (cross-linker in biosensor development), that usually leads to a decrease in enzyme activity. Thus, by an oxygen minisensor study an almost 2.5-fold decrease of the enzyme activity in the presence of GLU was detected, see ESI, Fig. S5. This effect is



**Table 2**  
Impact of deposition parameters on the performance of one-pot/one-electrode nanobiosensors.

| Liner detection range (LDR)/ and detection limit (LOD) | Design   |  |
|--|--|--|
|  | A: 1-st level: Pd-NPs -2.5 mA 30 s<br>2-d level: Pd/LOx/Naf -2.5 mA 30 s<br>3-d level: Pd/GOx/Naf -2.5 mA 30 s | B: 1-st level: -5 mA 120 s<br>2-d level: Pd/LOx/Naf -2.5 mA 30 s<br>3-d level: Pd/GOx/Naf -2.5 mA 30 s |
|  |                               |                     |
| H <sub>2</sub> O <sub>2</sub> , LDR, mM                | 0.02 – 100 mM  | 1 – 100 mM   |
| LOD, μM  | 7 ± 2 μM   | 180 ± 20 μM  |
| Glucose, LDR, mM                                       | 0.2 – 50 mM  | 1 – 15 mM  |
| LOD, μM  | 100 ± 10 μM  | 500 ± 45 μM  |
| Lactate LDR, mM  | 0.5 – 2 mM   | 1.5 – 2 mM   |
| LOD, μM  | 250 ± 20 μM  | 850 ± 85 μM  |

completely eliminated in our electroplated tailored nanobiosensors regardless their architecture. Additionally, the proposed concept of sequential immobilization of enzymes by electroplating from multiple electrolyte solutions does not suffer from competitive behavior of the multiple bioreceptors during their attachment to the active sites of cross-linker agents, typically seen for a covalent simultaneous co-immobilization of several free enzymes from the cocktail mixture on the same electrode [11–13].

### 3.5. The operating of one-pot/one-electrode nanobiosensor beyond the enzymatic sensing: glutaraldehyde detection

#### 3.5.1. Performance and operating

The absence of glutaraldehyde (GLU) in the design of one-pot/one-electrode nanobiosensors makes its separate detection as an

environmental pollutant and important analyte in cells-related experiments possible [21].

To this end, after deactivation of enzymes (sensor was heated to 65 °C for 1 h) our one-pot/one-electrode nanobiosensor was tested in CV mode with GLU (Fig. 7A). A significant current increase was detected with GLU at the potential of 0.12 V and pH 10. The calibration curve recorded at the applied potential of 0.12 V in AM mode exhibited a wide dynamic range, viz. LDR = 1 – 100 mM with regression coefficient  $R^2 = 0.971$  (Fig. 7B). The detection limit (S/N = 3) was determined at the level of  $200 \pm 10 \mu\text{M}$ .

More significantly, our experiments revealed that after testing of this modular one-pot/one-electrode nanobiosensor in AM mode with GLU at pH 10 it is possible to further explore this sensor again to detect H<sub>2</sub>O<sub>2</sub> at pH 7. Thus, the oxidation of GLU conducted at pH 10 by one-pot/one-electrode nanobiosensor did not result in any irreversible changes in

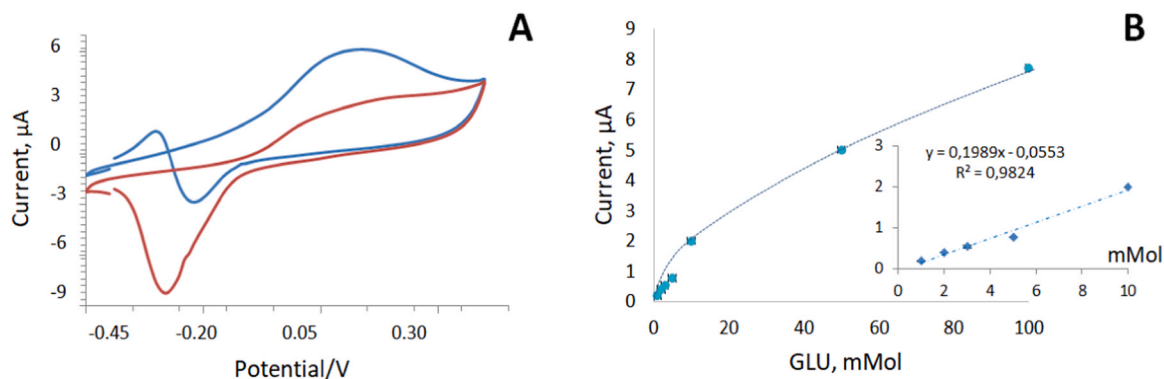


**Fig. 7.** Cyclic voltammetry (CV) curves recorded at 20 mV/s from a modular one-pot/one-electrode nanobiosensor (A): red – in a phosphate buffer, pH 10; blue – 100 mM GLU solution, pH 10. Calibration curve for GLU at pH 10 obtained in AM mode at the applied potential of 0.12 V (B). (For interpretation of the references to color in this figure legend, the reader is referred to the web version of this article.)

the structure and sensing properties of Pd-NPs-doped OIH. In other words, no irreversible changes in sensor structure occur that makes their manufacturing attractive for modular cyclic catalysis.

### 3.5.2. Specific regeneration procedure after glutaraldehyde sensing

Successful regeneration of the sensor surface is crucial for its cyclic, continuous usage or integration into microfluidic devices [22]. For this goal, we developed a multi-step procedure (see Section 3.2.1 “Impact of nanobiosensor composition and polarization mode”) to regenerate the intact surface of Pd-NPs-based nanobiosensor and its basic line for the detection of  $\text{H}_2\text{O}_2$  as an individual component or as a product of oxidases activity (GOx or LOx). This procedure helped to maintain the basic line of nanobiosensor after a continuous usage at the level of 95–99% as compared to the signal obtained from as-fabricated device. However, after the usage of nanobiosensor to detect 100 mM GLU at pH 10 the basic line of the sensor was found to retrieve ~79.4% of the signal obtained from an as-fabricated sensor in buffer solution at neutral pH. This result is explained by the extensive formation of Pd surface oxides triggered by GLU oxidation at alkaline media [23].

For a deep regeneration process of the modular Pd-NPs-based sensor, we developed the cleaning protocol with the goal of recovering the initial basic line at the applied potential of 0.2 V in MAM mode. A cleaning process was optimized for a Pd-NPs-doped nanoelectrode by treating its surface in buffer at pH 7 in the following two-step amperometric sequence: at  $-0.2$  V for 180 s followed by signal recording at 0.2 V for 30 s. This procedure was found to be sufficient to remove the majority of the formed Pd-oxides at the surface. At the applied cleaning conditions (single cleaning) the electrical current measured at the potential of 0.2 V was found to recover ~98% of the original current obtained before GLU sensing in AM mode at pH 10 (see ESI, Table S1). Hence, this procedure makes the detection of  $\text{H}_2\text{O}_2$  (pH 7) possible again even after GLU sensing performed at pH 10. The cyclic experiment by switching between GLU (AM mode, pH 10) and  $\text{H}_2\text{O}_2$  (MAM mode, pH 7) detection was repeated at least 10 times with the same analytical performance for both analytes.

### 3.6. Summarized guidelines of modular one-pot/one-electrode

The modularity, specificity and sensitivity of the modular biosensing is based on the switching between the modules towards sensing of the targeted analyte without signal interference raised by different immobilized functional layers [24]. In our case the specific detection of bio-analyte is triggered by an immobilized type of oxidase operated at the switchable electrochemical read-out mode at pH 7, see ESI, Fig. S6. After deactivation of enzymes (due to the usage of solutions with aggressive pH, storage at high temperatures or conventional aging process), a facile analysis of hydrogen peroxide and glutaraldehyde in a wide concentration range by the same one-pot/one-electrode nanobiosensor appears to be possible.

Importantly, to distinguish the signal between pure  $\text{H}_2\text{O}_2$  decomposition as the targeted analyte (TA) and  $\text{H}_2\text{O}_2$  as a product (P) of enzymatic activity (during lactate and glucose sensing) the basic line, calibration curves and LDRs obtained for individual  $\text{H}_2\text{O}_2$ , glucose and lactate on the same sensor should be taken into account, Fig. 8.

Hence, the detection of  $\text{H}_2\text{O}_2$  as a TA or P by the same sensor and read-out mode occurs on different current levels. This is because the amount of pure 2 mM (as example)  $\text{H}_2\text{O}_2$  solution loaded on the sensor is always higher than  $\text{H}_2\text{O}_2$  amount released during specific enzymatic reaction between immobilized GOx and 2 mM of glucose. However, to this end, the reproducibility of one-pot/one-electrode synthesis and its calibrations from a similar batch should be very high. Our sensors meet this requirement, see ESI, Table S2.

To conclude, the calibration of one-pot/one-electrode nanobiosensors should be performed at different pH and electrochemical modes: at pH 7 in multi-step potentiostatic mode at the applied potentials of 0.2 V for 30 s (step 1) and at  $-0.08$  V for 60 s (step 2) for  $\text{H}_2\text{O}_2$ ,

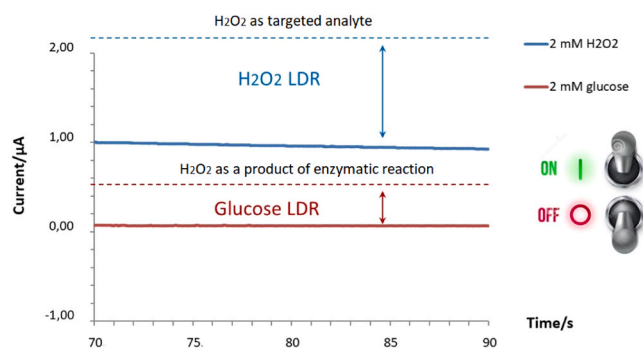


**Fig. 8.** MAM curves (polarization at  $-0.08$  V, signal read-out at 0.2 V) recorded from the modular Pd-NPs-doped one-pot/one-electrode for the same concentration of targeted analyte. Note: the electrochemical read-out for oxidase-containing nanobiosensors (glucose and lactate detection) is the same as it is used for separate  $\text{H}_2\text{O}_2$  analysis (as a targeted analyte) but occurs on different current levels (in this design linear dynamic range, LDR, for glucose 200  $\mu\text{M}$  – 50 mM; LDR for hydrogen peroxide 20  $\mu\text{M}$  – 100 mM; the detection limits ( $S/N = 3$ ) were  $100 \pm 12$  and  $7 \pm 2$   $\mu\text{M}$  for glucose and hydrogen peroxide, respectively). This allows us to conduct a separate detection of individual analytes (i.e. glucose followed by hydrogen peroxide) in a sequential manner by a single electrode according to the proposed operational guidelines, see ESI, Fig. S6. “ON/OFF” option indicates the switching between the electrochemical detection modes, basic lines and LDRs (shown for basic lines and LDRs as a case study).

D-glucose and L-lactate detection (selectivity towards a specific bio-analyte detection is achieved by the immobilized oxidase type, i.e. LOx or GOx), and in conventional amperometric mode at 0.12 V and pH 10 for glutaraldehyde (GLU) analysis.

The next step in this research will be the developing of special protocols to explore and to validate the proposed system in the presence of all targeted analytes in the mixtures, evaluation of matrix effects and developing the guidelines to eliminate or minimize them.

## 4. Conclusions

In this study, by accurate tuning of nanoparticles design and technological compromise between their 3D-structure protecting enzymes from the non-controlled leakage and, at the same time, providing their release, Pd-NPs-doped one-pot/one-electrode electroplated amperometric nanobiosensor was constructed. The developed one-pot/one-electrode nanobiosensor allows advanced multiplex analyte detection, viz. L-lactate, D-glucose, hydrogen peroxide and glutaraldehyde. The modularity was achieved by means of the applied electrochemical read-out mode, pH and type of encapsulated enzyme. The synthesis of the hybrid Pd-NPs-doped one-step/one-electrode nanobiosensor for modular catalysis is a fully instrumentally controlled process allowing producing of the templates with tailored morphology and surface chemistry. Finally, the optimized regeneration procedure of the hybrid one-pot/one-electrode enables long-term monitoring of glutaraldehyde and hydrogen peroxide in different electrochemical modes without any significant loss in sensor sensitivity at least up to 10 cycles.

The obtained knowledge on electroplated nanodevice engineering, electrochemistry, bioanalytical chemistry and sensing approaches can significantly contribute to future strategies employed in nanobioengineering.

### CRedit authorship contribution statement

**Marcus Koch:** took part in the development of the template-assisted engineering concept, performed all SEM and TEM studies, data visualization and analysis, drafted several parts of the original manuscript, Formal analysis, writing, review. **Nina Apushkinskaya:** conducted sensor-related experiments, data visualization, Formal analysis.



**Ekaterina V. Zolotukhina:** was responsible for the Conceptualization and design of electrochemical experiments, Data analysis, Writing, reviewing, and editing of the manuscript. **Yuliya E. Silina:** conceptualized the concept of the research, was responsible for the design of the manuscript, Project administration, wrote, reviewed, and edited the manuscript, Funding acquisition, Project administration, Conceptualization, Writing - review & editing.

#### Declaration of Competing Interest

The authors declare that they have no known competing financial interests or personal relationships that could have appeared to influence the work reported in this paper.

#### Acknowledgments

This study was a part of the research program of Y.E.S. funded by the Deutsche Forschungsgemeinschaft (DFG, German Research Foundation, project 427949628). The authors would like to thank the German-Russian Interdisciplinary Science Center (G-RISC) for the support of collaboration between University of Saarland (Germany) and Institute of Problems of Chemical Physics RAS (Moscow region, Russia). E.V.Z. performed her work within the framework of the State assignment (number AAAA-A19-119061890019-5). Y.E.S. also thanks Jörg Schmauch (University of Saarland, Department of Experimental Physics) for the sputtering of Pd-foil and Prof. Dr. Bruce Morgan (University of Saarland, Institute for Biochemistry) for continuing support of this research at the department.

#### Appendix A. Supporting information

Supplementary data associated with this article can be found in the online version at [doi:10.1016/j.bej.2021.108132](https://doi.org/10.1016/j.bej.2021.108132).

#### References

- [1] B. Wang, M. Barahona, M. Buck, A modular cell-based biosensor using engineered genetic logic circuits to detect and integrate multiple environmental signals, *Biosens. Bioelectron.* 40 (2013) 368–376, <https://doi.org/10.1016/j.bios.2012.08.011>.
- [2] R. Wang, B.F. Cress, Z. Yang, J.C. Hordines, S. Zhao, G.Y. Jung, Z. Wang, M.A. G. Koffas, Design and characterization of biosensors for the screening of modular assembled naringenin biosynthetic library in *Saccharomyces cerevisiae*, *ACS Synth. Biol.* 8 (2019) 2121–2130, <https://doi.org/10.1021/acssynbio.9b00212>.
- [3] A. Giannakopoulou, M. Patila, K. Spyrou, N. Chalmpes, D. Zarafeta, G. Skretas, D. Gournis, H. Stamatis, Development of a four-enzyme magnetic nanobiosensor for multi-step cascade reactions, *Catalysts* 9 (9) (2019) 955, <https://doi.org/10.3390/catal9120995>.
- [4] G. Jarockyte, V. Karabanovas, R. Rotomskis, A. Mobasheri, Multiplexed nanobiosensors: current trends in early diagnostics, *Sensors* 20 (2020) 1–23, <https://doi.org/10.3390/s20236890>.
- [5] N. Mano, *Engineering Glucose Oxidase for Bioelectrochemical Applications*, 128, Elsevier, 2019, pp. 218–240.
- [6] B. Hassler, R.M. Worden, A. Mason, P. Kim, N. Kohli, J.G. Zeikus, M. Laivenieks, R. Ofoli, Biomimetic interfaces for a multifunctional biosensor array microsystem, *Proc. IEEE Sens.* 2 (2004) 991–994, <https://doi.org/10.1109/icsens.2004.1426339>.
- [7] I. Moser, G. Jobst, G.A. Urban, Biosensor arrays for simultaneous measurement of glucose, lactate, glutamate, and glutamine, *Biosens. Bioelectron.* 17 (4) (2002) 297–302, [https://doi.org/10.1016/S0956-5663\(01\)00298-6](https://doi.org/10.1016/S0956-5663(01)00298-6).
- [8] R.M. Iost, F.N. Crespilho, Layer-by-layer self-assembly and electrochemistry: applications in biosensing and bioelectronics, *Biosens. Bioelectron.* 31 (1) (2012) 1–10, <https://doi.org/10.1016/j.bios.2011.10.040>.
- [9] K. Ariga, Q. Ji, J.P. Hill, Enzyme-Encapsulated layer-by-layer assemblies: current status and challenges toward ultimate nanodevices, *Adv. Polym. Sci.* (2010) 51–87, <https://doi.org/10.1007/12-2009-42>.
- [10] P. Vadgama, Multifunctional biosensor development and manufacture, in: *Comprehensive Biotechnology*, second ed., vol. 5, 2011, pp. 159–172, <https://doi.org/10.1016/B978-0-08-088504-9.00453-0>.
- [11] I. Wheeldon, S.D. Minter, S. Banta, S.C. Barton, P. Atanassov, M. Sigman, Substrate channelling as an approach to cascade reactions, *Nat. Chem.* 361 (2016) 299–3309, <https://doi.org/10.1038/nchem.2459>.
- [12] Y.H.P. Zhang, Substrate channeling and enzyme complexes for biotechnological applications, *Biotechnol. Adv.* 108 (1) (2011) 22–330, <https://doi.org/10.1016/j.biotechadv.2011.05.020>.
- [13] L. Poshyvailo, E. Von Lieres, S. Kondrat, Does metabolite channeling accelerate enzyme-catalyzed cascade reactions? *PLoS One* 12 (2017) 1–17, <https://doi.org/10.1371/journal.pone.0172673>.
- [14] D. Semenova, K.V. Gernaey, B. Morgan, Y.E. Silina, Towards one-step design of tailored enzymatic nanobiosensors, *Analyst* 145 (2020) 1014–31024, <https://doi.org/10.1039/c9an01745c>.
- [15] E.V. Butyrskaya, N. Korkmaz, E.V. Zolotukhina, V. Krasniukova, Y.E. Silina, Mechanistic aspects of functional layer formation in hybrid one-step designed GOx/Nafion/Pd-NPs nanobiosensors, *Analyst* 146 (2021) 2172–32185, <https://doi.org/10.1039/d0an02429e>.
- [16] P. Yáñez-Sedeño, A. González-Cortés, S. Campuzano, J.M. Pingarrón, Multimodal/multifunctional nanomaterials in (Bio)electrochemistry: now and in the coming decade, *Nanomaterials* 10 (2020) 1–64, <https://doi.org/10.3390/nano10122556>.
- [17] Y.E. Silina, D. Semenova, B.A. Spiridonov, One-step encapsulation, storage and controlled release of low molecular weight organic compounds: via electroplated nanoparticles, *Analyst* 144 (2019) 5677–5681, <https://doi.org/10.1039/c9an01246j>.
- [18] Y.E. Silina, B. Morgan, LDI-MS scanner: laser desorption/ionization mass spectrometry-based biosensor standardization, *Talanta* 223 (Pt 1) (2021), 121688, <https://doi.org/10.1016/j.talanta.2020.121688>.
- [19] K.V. Gor'kov, N.V. Talagaeva, S.A. Kleinkova, N.N. Dremova, M.A. Vorotyntsev, E. V. Zolotukhina, Palladium-polyppyrrrole composites as prospective catalysts for formaldehyde electrooxidation in alkaline solutions, *Electrochim. Acta* 345 (2020), 136164, <https://doi.org/10.1016/j.electacta.2020.136164>.
- [20] Y. Itoh, Y. Ohashi, T. Shibue, A. Hayashi, S. Maki, T. Hirano, H. Niwa, Reduction in desorption mass spectrometry: multiple protonation on flavins without charge increment, *J. Mass Spectrom. Soc. Jpn.* 50 (2002) 52–57, <https://doi.org/10.5702/masspec.50.52>.
- [21] A.O. Konakov, N.N. Dremova, I.I. Khodos, M. Koch, E.V. Zolotukhina, Y.E. Silina, One-pot synthesis of copper iodide-polyppyrrrole nanocomposites, *Chemosensors* 9 (3) (2021) 56, <https://doi.org/10.3390/chemosensors9030056>.
- [22] S.R. Shin, T. Kilic, Y.S. Zhang, H. Avci, N. Hu, D. Kim, C. Branco, J. Aleman, S. Massa, A. Silvestri, J. Kang, A. Desalvo, M.A. Hussaini, S.K. Chae, A. Polini, N. Bhise, M.A. Hussain, H.Y. Lee, M.R. Dokmeci, A. Khademhosseini, Label-free and regenerative electrochemical microfluidic biosensors for continual monitoring of cell secretomes, *Adv. Sci.* 4 (2017) 1–14, <https://doi.org/10.1002/advs.201600522>.
- [23] T. Schalow, B. Brandt, D.E. Starr, M. Laurin, S. Schaueremann, S.K. Shaikhutdinov, J. Libuda, H.J. Freund, Oxygen-induced restructuring of a Pd/Fe<sub>3</sub>O<sub>4</sub> model catalyst, *Catal. Lett.* 107 (2006) 189–196, <https://doi.org/10.1007/s10562-005-0007-5>.
- [24] A. Quijano-Rubio, H.W. Yeh, J. Park, H. Lee, R.A. Langan, S.E. Boyken, M.J. Lajoie, L. Cao, C.M. Chow, M.C. Miranda, J. Wi, H.J. Hong, L. Stewart, B.H. Oh, D. Baker, De novo design of modular and tunable protein biosensors, *Nature* 591 (2021) 482–487, <https://doi.org/10.1038/s41586-021-03258-z>.